

# Design and Analysis of a Self-Adaptive Monorail Transporter without Power Supply

Bao Zhou, Rui Hu, Miao He\*, Yujin Wang, and Hui Jin

College of Mechanical Engineering, Chongqing University of Technology, Chongqing 400054, China

\*Corresponding author e-mail: hemiaoj991@cqut.edu.cn

**Keywords:** Transporter, no power supply, adaptive function.

**Abstract:** An unpowered monorail transporter with self-adaptive function is proposed, which can convey crops downward at a relatively stable speed in mountainous regions. The monorail transporter is composed of the body, guiding mechanism, damping mechanism, braking mechanism, etc. Through the combination of compression spring, torsion spring and linear bearing, the transporter can adapt itself to the track passively and adjust its speed self-adaptively. The mechanical structure is designed in the paper firstly, and then the functional relationship between the speed and the stiffness of springs and the track parameters is obtained through the analysis of the kinematics and turning performance. Furthermore, a virtual simulation model is established to verify the reasonableness of the mechanical structure design and the analysis process.

## 1. Introduction

The problem of ageing population is faced by the world, especially for the developing countries dominated by agriculture. The large amount outflow of middle-aged population results the lacking of labor in rural, therefore, the low efficiency of the agricultural production. Additionally, human and animal-drawn transports are ubiquitous in mountainous regions, due to the difficult and the high cost of transportation facilities construction. That, in turn, would decrease the agricultural efficiency and also impede the economic development. Thus, the mechanization of agriculture conveying is very important for the increasement of farmers' income and agricultural economic development.

In order to solve the transportation problem in mountainous regions, researchers have developed many kinds of transporter, including the aerial ropeway conveyer, wheeled tractor, crawler vehicle, double-rail transporter, monorail transporter, and so on [1,2]. The aerial ropeway type of transportation is not restricted by the topography and climate [3]; however, it is inconvenient to maintain while it fails to work. The wheeled tractor [4] and crawler vehicle [5,6] are mainly used for the situations of heavy load and gentle slope. Furthermore, they require to pave special road, which is difficult in mountainous regions. The monorail transportation has advantages of lower construction and maintenance costs, small space occupation, flexible movement, comparing with the double-rail transportation and the others. As the result, the monorail transporter is widely used in agricultural transportation.

The monorail transporter meets the requirements of working in mountainous regions, due to the favorable adaptation of the switchback terrain. Then, there are a large amount of monorail transporters exist in literature. For example, J F Zhang et al [7] have developed a remote-control monorail transporter for mountainous orchard, which can climb up the slope no more than  $38^\circ$  with a load of 300 kg. Y Liu et al [8] developed a battery-drive monorail transporter with the ability to monitor its location. However, the monorail transporters reported in literature are driven by electric motor, diesel engine, and other driven approach. That may go against the usage in the remote areas where has no electric power supply and also lack professional maintenance personnel. Even worse, the power used by transporters may pollute the environment by releasing harmful gas.

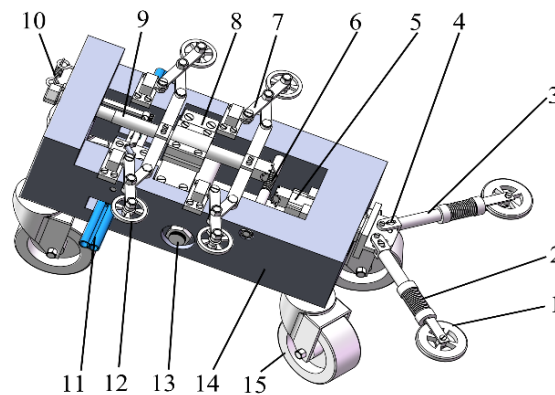
Thus, this paper is aim to design a self-adaptive monorail transporter without power supply, which can be used to convey the farm products from the peak to bottom in harvest season. This paper is organized as follows. The mechanical structure of the transporter is introduced in section 2, followed

by the linear motion analysis described in section 3. The analysis of turning radius is presented in section 4. Section 5 mainly reports the simulation process and the results of the monorail transporter using ADAMS. The conclusion is presented in section 6, followed by the acknowledgement.

## 2. Structure Design of the Self-Adaptive Monorail Transporter

The self-adaptive monorail transporter without power supply is mainly composed by main body, guide mechanism, damping mechanism, braking mechanism and rolling wheels. The mechanical structure model of the transporter is shown as Figure 1.

The guide wheels installed in the front of the guide mechanism can tightly contact with the interior wall of the monorail with the efforts of the compression springs. Cooperating with the width adjust nuts, the guide mechanism could be adapted to monorails with different width, even though there are large manufacturing errors. Meanwhile, the omni-directional wheels equipped under the main body makes the transporter has the ability of turning passively. Then, it can turn on the monorail due to the guide mechanism and the omni-directional wheels.



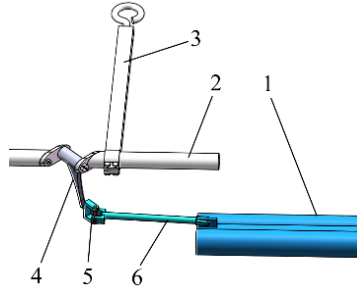
1—guide wheel; 2—compression spring; 3—guide rod; 4—width adjust nut; 5,8—sliding bearing; 6—torsion spring; 7—damping mechanism; 9—center shaft of the damping mechanism; 10—hand brake spring; 11—hand braking mechanism; 12—friction wheel; 13—load rod; 14—main body; 15—rolling wheel

Figure 1. Mechanical structure model of the transporter.

The shaft of the guide mechanism and the center shaft of the damping mechanism are installed in the main body by means of sliding bearings. Whereupon, the two shafts may have an opposite slide movement, due to the connection of them using torsion spring.

The damping mechanism is based on scissors mechanism, whose fixed rod is bolted on the main body while the removable rod is bolted on the center shaft of the damping mechanism. In this way, the damping mechanism may extend or shrink along with the width direction of the monorail. And then, the forces of the monorail interior wall on the friction wheels equipped at the end of scissors mechanism will increase or decrease as the transporter move along the monorail. When the monorail becomes broad, the guide mechanism will slide forward while the center shaft of the damping mechanism slides backward. This makes the friction wheels press upon the monorail interior wall tightly, therefore, increase the force of friction and decelerate the transporter. On the contrary, the transporter will accelerate along the monorail.

The braking mechanism ensures the transporter be effective while there are multiple working points along the monorail. When the worker pulls the string attached to the hand brake spring, the hand braking mechanism will expand and compact the interior wall of the monorail. Then, the transporter may stop at this working point except as the worker pulls the string again. The braking mechanism based on slider-rocker mechanism [9] is shown as Figure 2.



1—slider; 2—rotation axis; 3—shank; 4—rocker; 5—crosshead pin bearing; 6—connecting rod

Figure 2. The braking mechanism.

### 3. Linear Motion Analysis

#### 3.1 The Analytical Model

The mechanical structure transporter is symmetrical about the center shaft, resulting the same force condition of the four friction wheels during the linear movement. Then the analytical model of the linear motion could be shown as Figure 3.

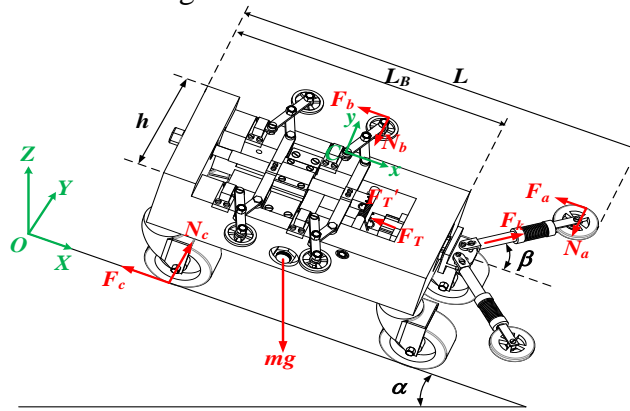


Figure 3. Analytical model of the linear motion.

According to the analytical model, the dynamics equations could be established as

$$\begin{cases} mg \cos \alpha = 4N_c \\ mg \sin \alpha - (2F_a + 4F_b + 4F_c) = ma \end{cases} \quad (1)$$

where,  $F_a=N_a s_a$ ,  $F_b=N_b s_b$ ,  $F_c=N_c s_c$ .  $N_a$  and  $F_a$  separately represent the positive pressure and friction applied to the guide wheel,  $N_b$  and  $F_b$  separately represent the positive pressure and friction applied to the friction wheel,  $N_c$  and  $F_c$  separately represent the positive pressure and friction applied to the rolling wheel.  $s_a$ ,  $s_b$ ,  $s_c$  represent the friction coefficient of the guide wheel, friction wheel and rolling wheel, separately.  $m$  represents the total mass including the transporter and the load,  $g$  represents the gravitational acceleration,  $\alpha$  represent the gradient of the monorail,  $a$  represent the acceleration of the transporter.

#### 3.2 The Damping Mechanism

The damping mechanism is composed of friction wheels and scissors mechanism [10], whose fixed rod is bolted on the main body while the removable rod is bolted on the center shaft of the damping mechanism. Then the damping mechanism can be illustrated as Fig.4, where the point A and C represent the removable point and fixed point respectively. The removable rod is connected with the guide mechanism at the point A in series using the torsion spring. The displacement of point A is opposite to the shaft of the guide mechanism. Therefore, the damping mechanism will play a role of speed adaptive adjustment.

As shown as Figure 4, the force of the compression spring can be described as

$$F_k = k_a \Delta_s = \sqrt{F_a^2 + N_a^2} \quad (2)$$

Where,  $F_k$ ,  $k_a$ ,  $\Delta_s$  represent the force, stiffness and displacement of the compression spring, respectively.

Then, the force  $F_T$  applied at the tip of the torsion spring can be obtained

$$F_T = 2F_k \cos \beta = 2 \cos \beta \sqrt{F_a^2 + N_a^2} \quad (3)$$

Where,  $\beta$  is the angle between the guide rod and the shaft of the guide mechanism.

The removable point A will slide a displacement  $\Delta_A$  along with the center shaft of the damping mechanism, resulting from the  $F_T$ , and the displacement  $\Delta_A$  can be expressed as

$$\Delta_A = F_T l_T^2 / k_T \quad (4)$$

Where,  $k_T$ ,  $l_T$  represent the stiffness coefficient and the arm length of the torsion spring, respectively.

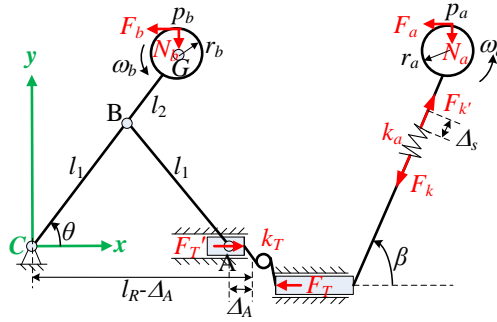


Figure 4. The model of the damping mechanism.

According to Figure 4, the coordinates of the center of the friction wheel marked as G should be described as

$$\begin{cases} x_G = (l_1 + l_2) \cos \theta = (l_1 + l_2) x_A / (2l_1) \\ y_G = (l_1 + l_2) \sin \theta = (l_1 + l_2) \sqrt{4l_1^2 - x_A^2} / (2l_1) \end{cases} \quad (5)$$

Where,  $l_1 = l_{AB} = l_{CB}$ ,  $l_2 = l_{BG}$ ,  $\cos \theta = x_A / (2l_1)$ , and  $x_A$  represents the coordinate of point A on the x-axis.

While the transporter moves at a uniform speed, it's in a force balance situation with the rolling wheels, friction wheels and also the guide wheels contacting with the monorail closely. We assume the width of the monorail is H, then

$$H = 2r_a + 2(l_{a0} - \Delta_{s0}) \sin \beta = 2r_b + h + (l_1 + l_2) \sqrt{4l_1^2 - x_{a0}^2} / l_1 \quad (6)$$

where,  $\Delta_{s0}$  represents the displacement of compression spring in the force balance situation;  $\Delta_{A0}$  and  $x_{A0}$  represent the corresponding displacement and coordinate of point A, respectively;  $l_{a0}$  represents the initial length of guide rod; h represents the body width;  $r_a$  and  $r_b$  represent the radius of guide wheel and friction wheel, respectively.

According to Eqs. (1)-(2), the acceleration of the transporter is  $a=0$  while it moves at a uniform speed. Then,  $F_a$  and  $\Delta_{A0}$  could be shown as

$$\begin{cases} F_a = k_a s_a \Delta_{s0} / \sqrt{s_a^2 + 1} \\ \Delta_{A0} = 2k_a \Delta_{s0} \cos \beta l_T^2 / k_T \end{cases} \quad (7)$$

And the relation between  $F_a$  and  $F_b$  could be obtained

$$mg (\sin \alpha - s_c \cos \alpha) = 2F_a + 4F_b \quad (8)$$

As the left of the equation above is constant, the change of  $F_b$  is opposite to the change of  $F_a$  which is related to the displacement of the compression spring. Thus, this transporter can adapt itself to the change of the width of the monorail caused by manufacturing or some other factors.

#### 4. Analysis of Turning Radius

The turning radius of the transporter is closely related to angle, width and the curvature radius of the curved monorail. When the curvature is greater than zero, the situation of the left guide wheel is different from the right, as shown as Figure 5. Where, the subscript l and r represent the left and right wheel, respectively.

The lengths of the left and right guide rod are equal to each other with the relationship of  $l_{al} = l_{ar} = l_{a0} - \Delta s_0$ , while the transporter works on the straight monorail. However, the situation changes on the curved monorail. For example, when the transporter turns right, the forces of the compression springs are that  $F_{kr} = k_a \Delta s_r$ ,  $F_{kl} = k_a \Delta s_l$  and  $F_{kr} > F_{kl}$ . Due to the displacement of the compression spring is in the range of  $0 \leq \Delta s \leq \Delta s_{max}$ , then the length of guide rod could be expressed as.

$$l_{a0} - \Delta s_{max} \leq l_a \leq l_{a0} \quad (9)$$

Additionally,  $l_{a0} - \Delta s_0 \leq l_{al} \leq l_{a0}$ ,  $l_{a0} - \Delta s_{max} \leq l_{ar} \leq l_{a0} - \Delta s_0$ , the turning angle of transporter is that  $0 \leq \gamma \leq \gamma_{max}$ , and

$$\gamma_{max} = \arccos \left\{ \left[ 4 \sin^2 \beta (l_{a0} - \Delta s_{max})^2 + (H - 2r_a)^2 - \Delta s_{max}^2 \right] / \left[ 2l_{ar} (H - 2r_a) \right] \right\} \quad (10)$$

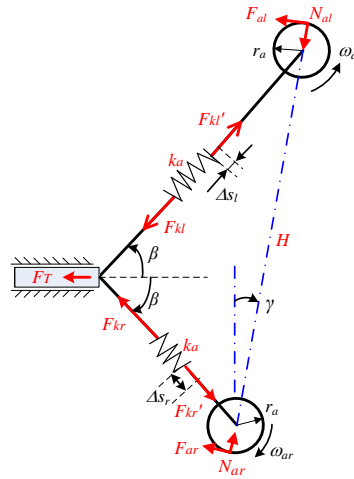


Figure 5. The diagram of the turning course.

Then the turning radius  $R$  could be derived out

$$R \geq L / [2 \sin(\gamma_{max} / 2)] \quad (11)$$

Where,  $L$  is the length of the transporter.

#### 5. Simulation Based on ADAMS

In order to verify the reasonableness of the mechanical structure design and the analysis process, the ADAMS software is used to simulate the transporter.

Firstly, the mechanical model of the transporter and also the monorail are established in SolidWorks software. And the parameters are shown as below:  $r_a = 20$  mm,  $r_b = 10$  mm,  $L = 360$  mm,  $L_B = 250$  mm,  $h = 80$  mm,  $H = 200$  mm,  $l_{a0} = 115$  mm,  $\Delta s_0 = 1.86$  mm,  $\beta = 45^\circ$ ,  $l_1 = l_2 = 25$  mm.

The operations of material attribute setting, interference checking, the setup of constraint conditions and motion parameters are made in SolidWorks after the modeling process. The duration time of the motion simulation is 1.0 s while the steps are set as 2000. Then, the displacement and

velocity of the center shaft of the damping mechanism are illustrated as Figure 6.

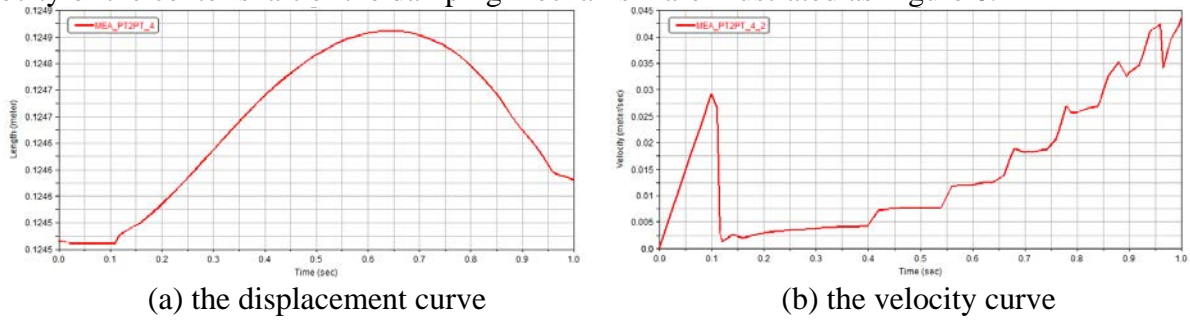


Figure 6. The displacement and velocity of the center shaft of the damping mechanism.

The displacement and velocity of the center of the friction wheel also could be obtained as shown as Figure 7.

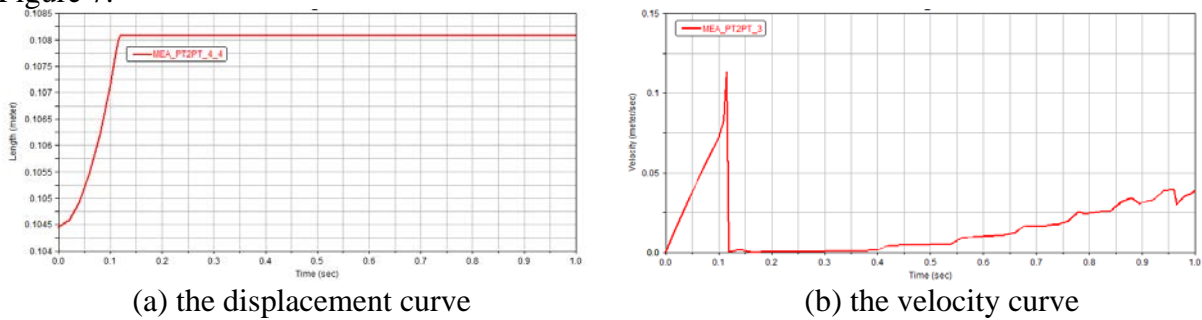


Figure 7. The displacement and velocity of the center of the friction wheel along y-axis.

As the removable rod of the scissors mechanism is bolted on the center shaft of the damping mechanism, then the displacement and velocity of the removable rod are equal to them of the center shaft of the damping mechanism that are shown as Figure 6. It can be seen from Figure 7, the displacement of the center of friction wheel along the y-axis is about 3.5 mm that could be regarded as the deformation of the rubber wheel. By the deformation of the rubber friction wheel, the friction force applied to transporter will increase and the self-adaptive capacity is achieved.

## 6. Conclusion

Mechanization and intellectualization are the trends of the agriculture in the world. With the aim to solve the agricultural transportation in mountainous region, a self-adaptive monorail transporter without power supply is designed in this paper, which can be used to convey the farm products from the peak to bottom in harvest season. The linear motion and turning radius are also analyzed through theoretical derivation. The transporter may play an important role in improving the efficiency and decreasing the labor intensity. However, the reliability, loading capacity and dynamics haven't be analyzed in this paper, which will be take into account in future.

## Acknowledgments

This work was supported by Scientific Research Foundation of Chongqing University of Technology (No. 2019ZD65), Project of Science and Technology Research Program of Banan District of Chongqing “The Research and Application of Modular Design Methodology for Agricultural Machinery based on Product Platform”.

## References

- [1] A Y Izmailov, Intelligent technologies and robotic means in agricultural production, Herald of the Russian Academy of Sciences, 89 (2019) 209-210.
- [2] K F Sanders, Orange harvesting systems review, Biosystems Engineering, 90 (2005) 115-125.

- [3] P Beňo, J Krilek, J Kováč, D Kozak, et al., The analysis of the new conception transportation cableway system based on the tractor equipment, *FME Transactions*, 46 (2018) 17-22.
- [4] M Ericson, Two-wheel tractors: Road safety issues in Laos and Cambodia, *Safety Science*, 48 (2010) 537-543.
- [5] J M Alcaraz, J Yamashita, K Sato, Development of a series hybrid-electric crawler farm transporter driving-range, energy consumption, and drivetrain efficiency, *Journal of the Japanese Society of Agricultural Machinery*, 71 (2009) 94-103.
- [6] T Nakata, Y Sogabe, T Araki, Vibration property of a rubber crawler system when traveling over bumps, *Engineering in Agriculture, Environment & Food*, 3 (2010) 47-53.
- [7] J F Zhang, Y L Zhang, T J Zhang, Design and improvement of the remote control traction monorail transporter, *Journal of Huazhong Agricultural University*, 32 (2013) 130-134.
- [8] Y Liu, Z Li, T S Hong, et al., Design of drive system for battery-drive monorail transporter for mountainous orchard, *Transactions of the Chinese Society of Agricultural Engineering*, 33 (2017) 34-40.
- [9] P A Simionescu, Design of planar slider-rocker mechanisms for imposed limit positions, with transmission angle and uniform motion controls, *Mechanism and Machine Theory*, 97 (2016) 85-99.
- [10] W Zhang, C Zhang, J B Zhao, et al., A Study on the static stability of scissor lift, *The Open Mechanical Engineering Journal*, 9 (2015) 954-960.